

Quantitative evaluation of deformable image registration based on TG-132

T. Ragul¹, V. Sharma², PV. Nameer⁴, SK Senthil Kumar⁴, Sumanta Manna¹, Sharad Singh², Pramod Kumar Gupta², Shaleen Kumar⁴, K J Maria Das³

¹ Department of Medical Physics, Kalyan Singh Super Specialty Cancer Institute, Lucknow, India

² Department of Radiation Oncology, Kalyan Singh Super Specialty Cancer Institute, Lucknow, India

³ Department of Physics, Lovely Professional University, Phagwara, Punjab, India

⁴ Department of Radiotherapy, Sanjay Gandhi Post Graduate Institute of Medical science, Lucknow, India

ABSTRACT

Aim: This study aimed to evaluate the Deformable Image Registration (DIR) software of Mirada® and Velocity® using quantitative measures as per the recommendation based on Task Group TG-132.

Materials and Methods: Task Group 132 has provided geometric and anatomic virtual phantoms for quality assurance, which were imported and contoured on the reference image, followed by DIR and then the contours were propagated on all the CT/CBCT data sets with different offsets and orientations of geometric and anatomic virtual phantom using Mirada and Velocity. Analysis was performed using the Dice Similarity Coefficient (DSC), Mean Distance to Agreement (MDA), Hausdorff (HD) and Target Registration Error (TRE). The results were compared to find the difference in significance using a paired t-test with a significance level of 5%.

Results: The obtained statistical result is listed below, considering the geometric phantom. With regards to DSC, Mean and SD values obtained for Mirada and Velocity are 0.955 ± 0.348 and 0.965 ± 0.418 , respectively with the p-value coming at 0.013 indicating a significant difference. Considering MDA, a significant difference of a p-value of 0.001 was found between Mirada and Velocity with the former having 0.668 ± 0.684 compared to 0.381 ± 0.424 for the latter. For HD, Mirada obtained a mean value of 3.464 ± 2.091 in comparison with 2.202 ± 1.215 for Velocity. As for TRE, three fiducials within the phantom were considered, and Mirada had a mean value of 1.037 mm while Velocity had 1.338 mm. While analysing the anatomic phantom, The DSC values for Mirada and Velocity were 0.946 ± 0.031 and 0.944 ± 0.313 respectively, indicating no significance. Similarly, no significance was found considering MDA (Mirada: 0.435 ± 0.235 , Velocity: 0.449 ± 0.242). Regarding HD, Mirada obtained 4.216 mm, while Velocity had 4.233 mm, showing exceptional compliance. The mean value of TRE for three fiducials was found to be less than 1 mm there has been a significant difference.

Conclusion: This study highlights the strengths and differences between Mirada and Velocity in DIR for adaptive radiotherapy. While both software applications excel in DSC, MDA and HD, the observed difference in TRE indicates a potential advantage of Mirada in achieving better image registration, especially in landmark-based registration scenarios.

Keywords: adaptive radiotherapy, deformable image registration, mirada, velocity, Dice Similarity Coefficient (DSC)

Address for correspondence:

Ragul T,

Medical Physicist/Scientist-I, Department of Medical Physics, Kalyan Singh Super Specialty Cancer Institute, Lucknow, India.

E-mail: ragul.at93@gmail.com@gmail.com

Word count: 3771 **Tables:** 02 **Figures:** 07 **References:** 27

Received: 03 May, 2024, Manuscript No. OAR-24-134237

Editor Assigned: 15 May, 2024, Pre-QC No. OAR-24-134237(PQ)

Reviewed: 20 May, 2024, QC No. OAR-24-134237(Q)

Revised: 25 May, 2024, Manuscript No. OAR-24-134237(R)

Published: 21 June, 2024, Invoice No. J-134237

INTRODUCTION

Deformable Image Registration (DIR) is a technique employed to monitor changes in a patient's anatomy throughout the course of radiotherapy. DIR entails aligning and registering images from multiple time points to construct a comprehensive representation of the patient's anatomy over time. Essentially, DIR calculates a deformation field that maps the pixels of one image to their corresponding pixels in another image. This deformation field is typically depicted as a 3D grid of vectors that describe the displacement of each pixel in one image to its corresponding pixel in the other image. The deformation field can then be utilised to transform one image to match the geometry of the other [1, 2]. Through the utilisation of DIR, medical professionals can more accurately identify and track changes in the patient's anatomy, encompassing alterations in size, shape, or location of the target tissue, as well as the growth of new tumours. This information can subsequently be leveraged to make more precise adjustments to the patient's treatment plan.

DIR boasts a plethora of applications in the realm of medical imaging, including adaptive radiotherapy, monitoring disease progression, image-guided surgery, and image segmentation [3-7]. Among its diverse applications, one of the most prominent is adaptive radiotherapy. Adaptive radiotherapy is a technique harnessed in radiation therapy to adjust the radiation dose and delivery during the treatment course, contingent on alterations in the patient's anatomy or tumour response. The primary objective of this technique is to enhance the effectiveness of radiation therapy while minimising the potential risk of side effects. Deformable Image Registration, which is a key component of adaptive radiotherapy, is highly effective in improving treatment outcomes for various types of cancer, such as lung, head and neck, and prostate cancers. Consequently, DIR plays a pivotal role in modern radiotherapy, as it facilitates the seamless integration of adaptive radiotherapy into clinical workflows. The American Association of Physicists in Medicine (AAPM). Task Group 132 has issued recommendations for the quantitative and qualitative assessment of DIR, with a focus on surface distance metrics and landmark analysis, along with associated supporting documentation. Numerous studies have already been published on the evaluation of the Deformation Vector Field-based (DVF) techniques [2]. Many prior studies in the field have primarily focused on individual metrics or were limited to the evaluation of a single software algorithm within virtual phantoms [8-14].

In our study, we have conducted a comparative analysis of two commercially available DIR algorithms, Mirada (Mirada Medical, Oxford, UK) and Velocity (Varian Medical Systems, Palo Alto, CA), with a particular emphasis on quantitative assessments like DSC, MDA, HD and TRE.

MATERIALS AND METHODS

Mirada and Velocity are widely used Deformable Image Registration (DIR) software tools. These applications facilitate the registration and fusion of images acquired from diverse modalities and at different time points while accounting for anatomical changes and deformations. Notably, Mirada employs a free-form deformation algorithm, whereas Velocity uses multi-resolution B-Spline algorithm [15, 16].

For quality assurance purposes, Task Group 132 has provided geometric and anatomic virtual phantoms [1], which were imported into both Velocity and Mirada. In this study, six datasets from the geometric phantoms were employed, comprising five CT and one CBCT dataset. The reference dataset, denoted as Basic Phantom Dataset-1 CT-Head First Supine (HFS), contains a cone pointing inferiorly, a semi-circle on the left side, and internal markers. Additionally, Basic Phantom Dataset-1 CBCT-HFS, Basic Phantom Dataset-2 (with offsets: To the left=1.0 cm, to anterior=0.5 cm, to superior=1.5 cm), Basic Phantom Dataset-3 (with offsets: To left=0.5 cm, To anterior=1.5 cm, to superior=2.0 cm, and rotations of 5 degrees along the X-axis, 8 degrees along

the Y-axis, and 10 degrees along the Z-axis). Basic Phantom Dataset-4 is the same as the reference dataset, except it's in Feet First Supine (FFS), while Basic Phantom Dataset-5 maintains the reference configuration except it's in a Head First Prone (HFP) position. Basic Phantom Dataset-6 retains the reference setup but is in a Feet First Prone (FFP) orientation [1].

In this study, three datasets from anatomic phantoms were also utilised, consisting of two CT and one CBCT datasets [1]. The reference dataset, termed Basic Anatomical Dataset-1 CT-HFS, contains a pelvis phantom with three markers in the regions of the bladder, prostate, rectum, and three skin markers. The Basic Anatomical Dataset-1 CBCT-HFS is used in parallel. Furthermore, the Basic Anatomical Dataset-2 replicates the reference CT dataset but introduces offsets (To the left = 0.3 cm, to anterior = 0.5 cm, to superior = 1.2 cm) For further information about virtual phantoms, please refer to the supplementary documents [17-25]. Experts manually delineated contours in all the phantom sets, including the reference CT dataset, for a total of 8 structures in both the geometric and anatomic phantoms. The study's workflow encompassed rigid registration, followed by DIR, and subsequently, the propagation of contours across all CT/CBCT datasets, with variations in offsets and orientations of geometric and anatomic virtual phantoms, using both Mirada and Velocity. Pre-implemented fiducials from the phantoms were employed for the evaluation of Target Registration Error (TRE) (Figures 1 and 2).

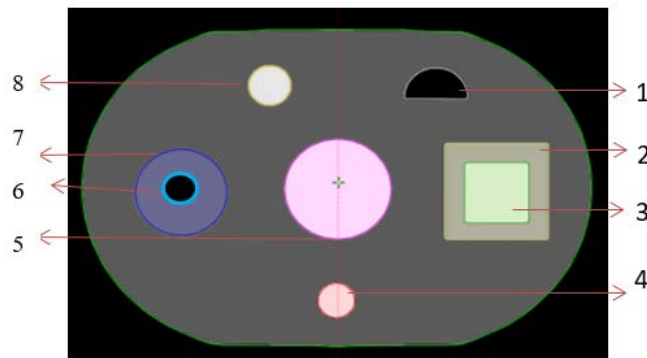


Fig. 1. Geometric Phantom 1. Anterior semicircle 2. Left outer square 3. Left inner square 4. Posterior circle 5. Central circle 6. Right Inner circle 7. Right outer circle 8. Anterior circle

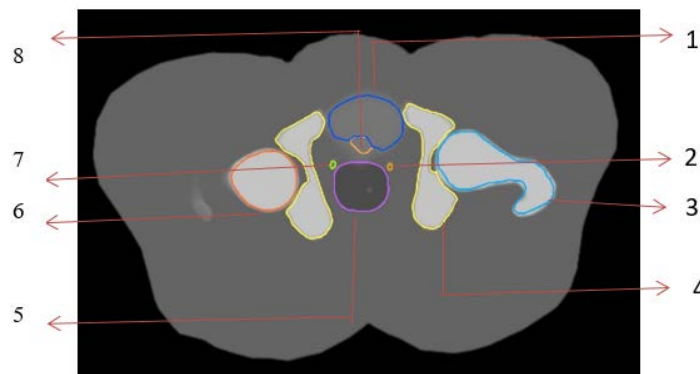


Fig. 2. Anatomic Phantom 1. Bladder 2. Left Seminal Vesicles 3. Left Femoral Head 4. Pelvic Bone 5. Rectum 6. Right Femoral Head 7. Right Seminal Vesicles 8. Prostate

DIR evaluation method

To conduct Quality Assurance (QA) for DIR, the delineated contours from the reference CT were propagated onto all the CT/CBCT datasets with various offsets and orientations. The accuracy of the registration can be assessed through the comparison of the propagated and manually delineated contours. In an ideal scenario with perfect registration and delineation, the propagated and manually delineated contours should perfectly overlap.

This evaluation is assessed using Surface Distance metrics such as (DSC), (MDA), and (HD).

Dice Similarity Coefficient (DSC)

DSC is a measure of the overlap between corresponding structures in the reference and registered images. Tolerance (0.8- 0.9) (Figure 3).

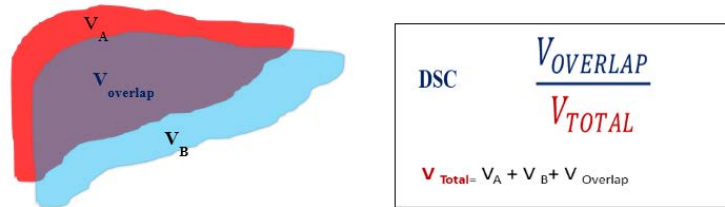


Fig. 3. Dice Similarity Coefficient (DSC)

Mean Distance to Agreement (MDA) and Hausdorff Distance (HD)

MSD is the average distance between the corresponding surfaces in the reference and registered images. It is calculated by first identifying the surface of interest in both images, and then computing

the distance between each point on the surface in the reference image and the closest point on the surface in the registered image. The distances are then averaged across all surface points. MDA <2 mm to 3 mm as per TG-132 (Figure 4). The maximum distance between all surface points is then taken as the HD.

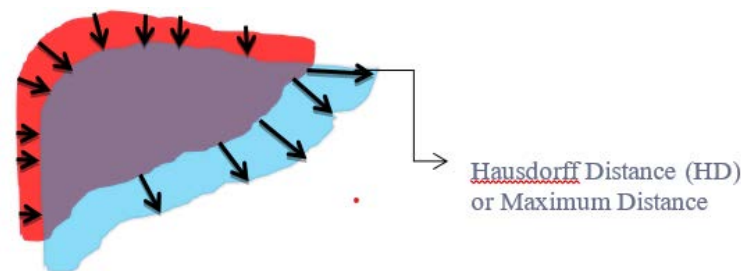


Fig. 4. Mean Distance to Agreement (MDA) and Hausdorff Distance (HD)

Target Registration Error (TRE)

The distance between the centroid of a fiducial or target in the

reference image and the centroid of the corresponding fiducial or target in the registered image TRE <2 mm–3 mm (Figure 5).

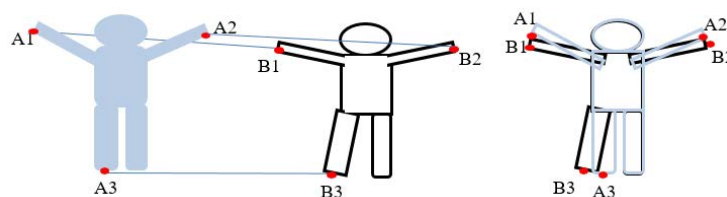


Fig. 5. Target Registration Error (TRE)

The Evaluation Process typically involves the following steps:

- Importing Propagated Structures: The first step is to import the structures generated by the two DIR algorithms with delineated structures.
- Quantitative Assessment: Once the structures are imported, the TG 132 QA evaluation module in Velocity calculates the DSC, MDA, and HD values. These metrics provide a comprehensive assessment of how well the Algorithms generated structures align with reference data or ground truth.

- For landmark-based evaluation like TRE is directly measured from the distance between the two fiducials after registration.

Inter algorithm variability

To determine inter-algorithm variability, the results were statistically grouped by the structures. The results were compared to find the difference in significance using paired t-test with a significance level set at 5%.

RESULTS

In our analysis of the geometric phantom, we focused on 8 distinct structures for examination. To ensure statistical rigour, a total of 48 samples were considered for the paired t-test. The resulting DSC means and Standard Deviation (SD) values for Mirada and Velocity were 0.951 ± 0.041 and 0.962 ± 0.035 , respectively. Significantly, the p-value was calculated to be 0.014, indicating a significant difference between these two software's. Moreover, when we considered the Mean Distance Agreement (MDA), a significant difference of p-value of 0.002 was observed between Mirada and Velocity. Mirada exhibited a mean MDA of 0.709 ± 0.705 , whereas velocity displayed a lower value of 0.411 ± 0.435 . For the HD, the data showed that Mirada achieved a mean value of 3.385 ± 2.150 , which was notably higher than the 2.190 ± 1.242 achieved by velocity.

In our analysis of TRE, we considered three fiducials within the phantom. Both Mirada and Velocity exhibited a mean and SD of 1.026 ± 1.384 . However, Velocity showed a slightly higher mean and SD at 1.344 ± 2.423 . The calculated p-value 0.031 shows no

statistically significant.

In the analysis of the anatomic phantom, we focused on eight distinct structures. This comprehensive examination involved a total of 16 samples for the t-test. For the DSC, the mean and SD values for both Mirada and Velocity were 0.946 ± 0.031 and 0.944 ± 0.313 , respectively. The calculated p-value of 0.312 suggests no statistically significant difference. Likewise, for the Mean Distance to Agreement (MDA), the results showed no significant distinction between Mirada 0.435 ± 0.235 and Velocity 0.449 ± 0.242 . The p-value for this comparison supports the absence of a significant difference. When considering the Hausdorff Distance (HD), Mirada yielded 4.233 ± 2.109 , while Velocity produced 4.233 ± 2.109 . The p-value of 0.751 indicates no significant difference between the two.

However, for the Target Registration Error (TRE), focusing on three fiducials, we observed a significant difference. The mean and SD values were 0.588 ± 0.224 for Mirada and 1.667 ± 0.871 for Velocity. The calculated p-value of 0.04 signifies a statistically significant difference in TRE between the two software programme (Table 1 and 2).

Tab. 1. Geometric phantom evaluation results

Test Name	Mean ± SD		p-Value
	Mirada	Velocity	
Dice Similarity Coefficient (DSC)	0.951 ± 0.041	0.962 ± 0.035	0.014
Mean Distance to Agreement (MDA) in mm	0.709 ± 0.705	0.411 ± 0.435	0.002
Hausdorff Distance (HD) in mm	3.385 ± 2.150	2.190 ± 1.242	0.0001
Target Registration Error (TRE)	1.026 ± 1.384	1.344 ± 2.423	0.031

Tab. 2. Anatomic phantom evaluation results

Test Name	Mean ± SD		p-Value
	Mirada	Velocity	
Dice Similarity Coefficient (DSC)	0.946 ± 0.031	0.944 ± 0.0313	0.312
Mean Distance to Agreement (MDA) in mm	0.435 ± 0.235	0.449 ± 0.242	0.257
Hausdorff Distance (HD) in mm	4.216 ± 2.084	4.233 ± 2.109	0.751
Target Registration Error (TRE)	0.588 ± 0.224	1.667 ± 0.8710	0.04

Tolerance: DSC: 0.8-0.9, MDA>2 mm, TRE: 2 mm-3 mm [1]

DISCUSSION

The present study undertook a comprehensive analysis of the performance of two Deformable Image Registration (DIR) software, Mirada and Velocity, in the context of image registration. Our investigation considered a range of quantitative metrics to assess the accuracy and reliability of these software applications. The results for the geometric phantom show that the mean Dice Similarity Coefficient (DSC) for Mirada is 0.951, and for velocity, it is 0.962. The values, which are closer to 1, indicate a high degree of overlap between the structures. so, velocity was performed slightly better in that the DSC test, there was the only exception, where velocity showed an out-of-tolerance for the Left Lateral Outer square structure 16 in the Basic Phantom Dataset-2, with a value

of 0.794, while Mirada showed 0.801 for the same structure (Figures 6 and 7).

By considering MDA the mean of all the structures within the tolerance (>2 mm) with the Mirada algorithm gives a mean value of 0.709 mm and velocity gives 0.411 it shows the velocity mean value was close to zero and performed better, at the case of Hausdorff Distance (HD) even though there was no tolerance given in the TG 132 in this study for Mirada, mean, HD value was around 3.385 mm and for velocity, it was 2.190 mm, where the maximum value is reached up to 9.481 mm in Mirada and velocity it reaches only up to 3.73 mm so the results clearly show that velocity performs better than the Mirada in surface distance metrics (Figure 7).

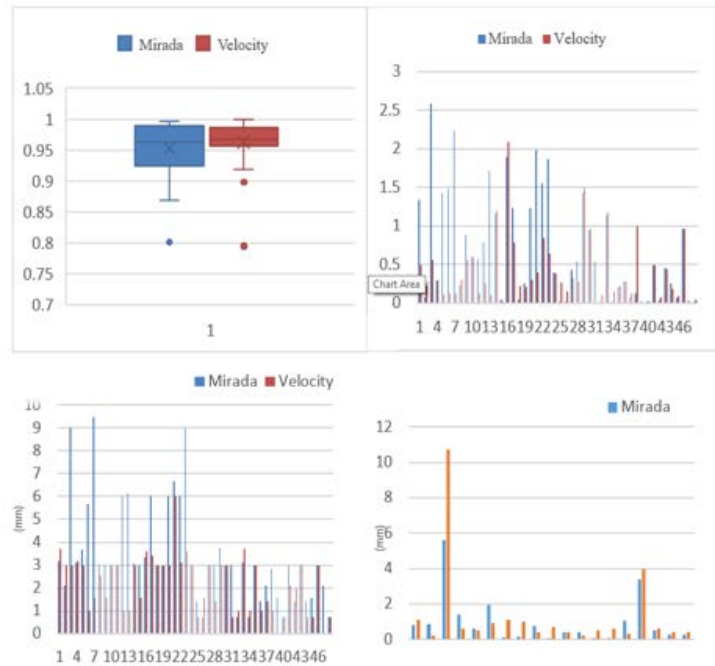


Fig. 6. Variation of Dice Similarity Coefficient (DSC), Mean Distance to Agreement (MDA), Housdroff Distance (HD), Target Registration Error (TRE) between Mirada and Velocity in Geometric Phantom

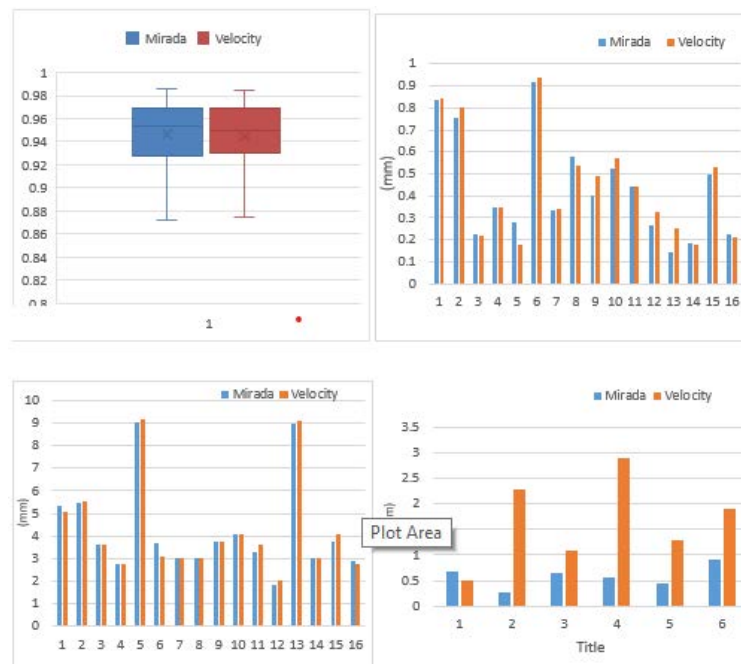


Fig. 7. Variation of Dice Similarity Coefficient (DSC), Mean Distance to Agreement (MDA), Housdroff Distance (HD), Target Registration Error (TRE) between Mirada and Velocity in Anatomic Phantom

In the analysis of the anatomic phantom, we examined eight distinct structures total of 16 samples, providing an evaluation of the software's ability to handle different anatomical regions. Notably, the DSC values for Mirada and Velocity are 0.946 ± 0.031 and 0.944 ± 0.0313 , respectively. These values, both close to 1, indicate a high degree of overlap between the structures in the evaluated images. Although the p-value of 0.312 suggests no significant difference between the two algorithms. This suggests that both software is capable of achieving a similar level of accuracy in contour propagation. The standard deviation values are 0.03 and 0.313 were very close, further supporting the consistency of their performance. Similarly, when examining the Mean Distance to Agreement

(MDA), our findings indicate that there is no significant difference between Mirada and Velocity. Both software applications exhibited comparable results, emphasising their reliability in capturing the spatial agreement between structures in the CT and CBCT datasets. The close mean values and standard deviations further substantiate the equivalence of their performance. The analysis of HD further confirmed the consistent performance of Mirada and velocity whose mean is 1.026 and 1.344 in the maximum goes up to 0.92 mm from Mirada and velocity is 2.2 mm. The HD values for both software applications were very close, with a calculated p-value that indicates no significant difference. This indicates that velocity exhibited a higher TRE compared to Mirada. While both software applications are capable of acceptable image registration,

this discrepancy in TRE suggests that Mirada may offer a better alignment of images in the case of landmark-based registration. The significance of this difference is particularly relevant in clinical scenarios where landmark or marker-based registration is critical. When evaluating the performance of the two algorithms, it is evident that there is a minimal gap in their effectiveness. The B-spline method, which utilises a grid of control points for image transformation and interpolates movements using cubic B-spline functions, generally ensuring a smoother deformation. On the contrary, the Demons approach, rooted in the optical flow method, may produce irregular deformations if not meticulously regularized. Despite historical advantages in processing time for Demons, recent advancements have significantly enhanced the speed of B-spline algorithms, making them competitive. There's been limited research on how well DIR algorithms in TPS systems handle CT-CT contour propagation. Hardcastle et al. found that fast symmetric Demons and Salient-Feature-Based Registration (SFBR) algorithms in Pinnacle TPS performed similarly to our study, with Dice coefficients are around 0.8 for various structures. Peroni et al. compared MIM with an open-source B-Spline algorithm and saw no significant differences. Hoffmann et al. reported less than 4 mm target registration error in 79% of cases with Velocity AI's B-spline-based algorithm. La Macchia et al. found no significant differences among ABAS, MIM, and Velocity AI. In our study, B-spline and Demons-based algorithms within popular treatment planning systems were compared. Although there were no significant differences between algorithms [26-27]. In summary, our study provides valuable insights into the perfor-

mance of Mirada and Velocity in deformable image registration for radiotherapy planning. While both software applications excel in contour propagation, spatial agreement, and HD, the observed discrepancy in TRE suggests that Mirada may have an advantage in achieving superior image registration, particularly in landmark-based registration scenarios. This specific observation adds a novel dimension to the comparative analysis. This study adds to the body of knowledge on the topic of adaptive radiotherapy by shedding light on the performance of these software tools in a context where precision and accuracy are of utmost importance.

CONCLUSION

This study highlights the strengths and differences between Mirada and Velocity in DIR for Adaptive Radiotherapy. While both software applications excel in DSC, MDA and HD, the observed difference in TRE indicates a potential advantage of Mirada in achieving better image registration, especially in landmark-based registration scenarios. Clinicians and medical physicists should carefully consider these findings when implementing DIR in clinical radiotherapy.

ACKNOWLEDGEMENT

I would like to express my sincere gratitude to Mr. Kangavel, PTW Dosimetry India Pvt Ltd for their invaluable assistance and guidance in this research endeavor.

REFERENCES

1. Brock KK, Sharpe MB, Dawson LA, Kim SM, Jaffray DA, et al. Use of image registration and fusion algorithms and techniques in radiotherapy: Report of the AAPM Radiation Therapy Committee Task Group No. 132. *Med Phys*. 2017;44:43-76.
2. Latifi K, Zhang GG, Hunt D, Moros EG, Samei E, et al. Practical quantification of image registration accuracy following the AAPM TG-132 report framework. *J Appl Clin Med Phys*. 2018 ;19:125-133.
3. Kumarasiri A, Siddiqui F, Liu C, Yecheili R, Shah M, et al. Deformable image registration based automatic CT-to-CT contour propagation for head and neck adaptive radiotherapy in the routine clinical setting. *Med Phys*. 2014;41:121712.
4. Nie K, Pouliot J, Smith E, Chuang C. Performance variations among clinically available deformable image registration tools in adaptive radiotherapy – how should we evaluate and interpret the result? *J Appl Clin Med Phys*. 2016;17:328-340.
5. Rigaud B, Simon A, Castelli J, Gobeli M, Ospina Arango JD, et al. Evaluation of deformable image registration methods for dose monitoring in head and neck radiotherapy. *Biomed Res Int*. 2015;2015:145160.
6. Fusella M, Giglioli FR, Fiandra C, Ragona R. Evaluation of dose recalculation vs dose deformation in a commercial platform for deformable image registration with a computational phantom. *Med Dosim*. 2018 Spring;43:82-90.
7. Chetty IJ, Rosu-Bubulac M. Deformable registration for dose accumulation. *Semin Radiat Oncol*. 2019;29:198-208.
8. Dou TH, Thomas DH, O'Connell DP, Lamb JM, Lee P, et al. A method for assessing ground-truth accuracy of the 5DCT technique. *Int J Radiat Oncol Biol Phys*.
9. Scaggion A, Farace P, Riboldi M, Baroni G. Free-to-use DIR solutions in radiotherapy: Benchmark against commercial platforms through a contour-propagation study. *Physica Medica*. 2020;74:110-117.
10. Lawson JD, Schreiber E, Jani AB, Fox T. Quantitative evaluation of a cone-beam computed tomography–planning computed tomography deformable image registration method for adaptive radiation therapy. *J Appl Clin Med Phys*. 2007;8:96-113.
11. Kirby N, Chuang C, Pouliot J. A two-dimensional deformable phantom for quantitatively verifying deformation algorithms. *Med Phys*. 2011;38:4583-4586.
12. Singhrao K, Kirby N, Pouliot J. A three-dimensional head-and-neck phantom for validation of multimodality deformable image registration for adaptive radiotherapy. *Med Phys*. 2014 ;41:121709.
13. Moseley JL, Brock KK, Sharpe MB, Dawson LA, Kim SM, Jaffray DA, et al. Validation of a Commercial DIR Algorithm for Dose Accumulation. *Int J Radiat Oncol Biol Phys*. 2016;96:615-616.
14. Lee S, Park H, Kim J.. Evaluation of hepatic toxicity after repeated stereotactic body radiation therapy for recurrent hepatocellular carcinoma using deformable image registration. *Sci Rep*. 2018;8:1-9.
15. Kubli A, Russo M, Van Schie G, Keesman R, Slotman BJ, et al. Variability in commercially available deformable image registration: A multi-institution analysis using virtual head and neck phantoms. *J Appl Clin Med Phys*. 2021;22:89-96.
16. Guy CL, Walker GV, Stingo FC, Tennyson N, Jan N, et al. Evaluation of image registration accuracy for tumor and organs at risk in the thorax for compliance with TG 132 recommendations. *Adv Radiat Oncol*. 2019;4:177-185.
17. Kashani R, Hub M, Balter JM. Objective assessment of deformable image registration in radiotherapy: a multi-institution study. *Med Phys*. 2008;35:5944-5953.
18. Klein S, Staring M, Murphy K, Viergever MA, Pluim JP. Elastix: a toolbox for intensity-based medical image registration. *IEEE Trans Med Imaging*. 2009;29:196-205.
19. Kadoya N, Nakajima Y, Saito M, Miyasaka Y, Otsuka K, et al. Evaluation of various deformable image registration algorithms for thoracic images. *J Radiat Res*. 2014;55:175-182.
20. Peroni M, Ciardo D, Riboldi M, Alterio D, Zaffino P, et al. Validation of automatic contour propagation for 4D treatment planning using multiple metrics. *Technol Cancer Res Treat*. 2013;12:501-510.
21. Loi G, Forlani A, Ronzoni M, Cavedon C, Baroni G, et al. Performance of commercially available deformable image registration platforms for contour propagation using patient-based computational phantoms: a multi-institutional study. *Med Phys*. 2018;45:748-757.
22. Bookstein FL. Principal warps: Thin-plate splines and the decomposition of deformations. *IEEE Trans Pattern Anal Mach Intell*. 1989;11:567-585.
23. Gering D, Nabavi A, Kikinis R, Hata N, O'Donnell L, et al. Image Deformation Based on a Marionette Model. *Med Phys*. 2010;37:3127-3127.
24. Rong Y, Rosu-Bubulac M, Benedict SH, Cui Y, Ruo R, et al. Rigid and Deformable Image registration for radiation therapy: a self-study evaluation guide for NRG oncology clinical trial participation. *Pract Radiat Oncol*. 2021;11:282-298.
25. Hardcastle N, Tomé WA, Cannon DM, Brouwer CL, Wittendorp PW, Dogan N, et al. A multi-institution evaluation of deformable image registration algorithms for automatic organ delineation in adaptive head and neck radiotherapy. *Radiat Oncol*. 2012;7:1-7.
26. La Macchia M, Fellin F, Amichetti M, Cianchetti M, Gianolini S, Paola V, et al. Systematic evaluation of three different commercial software solutions for automatic segmentation for adaptive therapy in head-and-neck, prostate and pleural cancer. *Radiat Oncol*. 2012;7:1-6.
27. Ciardo D, Peroni M, Riboldi M, Alterio D, Baroni G, et al. The role of regularization in deformable image registration for head and neck adaptive radiotherapy. *Technol Cancer Res Treat*. 2013 ;12:323-31.